

Abstract No. Yoon0398

## Investigation of the Local Structure of the $\text{LiNi}_{0.5}\text{Mn}_{0.5}\text{O}_2$ Cathode Material During Electrochemical Cycling by X-ray Absorption Spectroscopy

Won-Sub Yoon (SUNY and BNL), Clare P. Grey (SUNY), Xiao-Qing Yang, and James McBreen (BNL)

Beamline(s): X18B

**Introduction:** Layered lithium nickel manganese oxides have recently been shown to be promising positive electrode materials for use in lithium-ion rechargeable batteries.<sup>1,2</sup> Ohzuku et al. showed that lithium nickel manganese oxide represents a possible alternative to  $\text{LiCoO}_2$  for advanced lithium batteries, in terms of its operating voltage, capacity, cycleability, safety, and materials economy.<sup>1</sup> Lu et al. reported that  $\text{Li}[\text{Ni}_x\text{Li}_{(1/3-2x/3)}\text{Mn}_{(2/3-x/3)}]\text{O}_2$  with  $x = 1/3, 5/12,$  or  $1/2$  can be cycled between 2.0 and 4.6 V to give a stable capacity of about 200, 180, or 160 mAh/g, respectively, at room temperature. The DSC results showed good safety characteristics.<sup>2</sup> Kim et al. showed that the electrochemically inactive  $\text{Li}_2\text{TiO}_3$  component in their  $x\text{LiNi}_{0.5}\text{Mn}_{0.5}\text{O}_2 \cdot (1-x)\text{Li}_2\text{TiO}_3$  systems contributes to the stabilization of the  $\text{LiNi}_{0.5}\text{Mn}_{0.5}\text{O}_2$  electrodes.<sup>3,4</sup> In this paper, we apply *in situ* X-ray Absorption Spectroscopy (XAS) to examine the  $\text{LiNi}_{0.5}\text{Mn}_{0.5}\text{O}_2$  electrode system and probe the electronic and local structure around the Mn/Ni and Li atoms during the first charge and discharge processes. We establish the major charge compensation mechanisms in the  $\text{Li}[\text{Mn}_{0.5}\text{Ni}_{0.5}]\text{O}_2$  electrode system during electrochemical cycling and show that these materials are more disordered than implied by their nominal composition.

**Methods and Materials:**  $\text{LiNi}_{0.5}\text{Mn}_{0.5}\text{O}_2$  powders were synthesized by reacting stoichiometric quantities of a coprecipitated double hydroxide of manganese and nickel with lithium hydroxide at 900 °C for 24 h in  $\text{O}_2$ . XAS measurements were performed in the transmission mode at beamline 18B of the National Synchrotron Light Source (NSLS) using a Si(111) double-crystal monochromator detuned to 35 - 45% of its original intensity to eliminate the high order harmonics. The *in situ* Mn and Ni K-edge XAS data were obtained in two separate cells. Energy calibration was carried out by using the first inflection point of the spectrum of Mn and Ni metal foil as a reference (*i.e.*, Mn K-edge = 6539 eV and Ni K-edge = 8333 eV). Reference spectra were simultaneously collected for each *in situ* spectrum by using Mn or Ni metal foils.

**Results:** The XRD pattern of  $\text{LiNi}_{0.5}\text{Mn}_{0.5}\text{O}_2$  is consistent with a single phase with the  $\alpha$ - $\text{NaFeO}_2$  structure (Figure

1); all the reflections can be indexed by assuming the hexagonal axes setting of the rhombohedral  $R\bar{3}m$  space group. The 006/012 and the 108/110 pairs of reflections are well resolved, which is typical of a well developed layered structure.<sup>6</sup> The voltage profiles of the cell during the first charge and discharge for experiments performed at the Mn and Ni K-edges are shown in Figure 2. The cells were charged from their open circuit potentials up to 4.6 V and then discharged, at a constant current rate of C/20, calculated based on the theoretical capacity. The specific capacity was calculated from the elapsed time, current, and mass of the active material in the cathode, by assuming that all the current passed was due to lithium intercalation/deintercalation reaction. Two electrochemical processes are observed, the first one occurring at a potential of approximately 4V and a second at a lower potential of 1V. The electrochemical behavior of our electrode at 4 V is similar to that observed in earlier reports.<sup>1,2</sup> The lower voltage process has been recently reported by Johnson et al.<sup>4</sup>

Figure 3 shows some selected normalized Mn and Ni K-edge XANES spectra of  $\text{LiNi}_{0.5}\text{Mn}_{0.5}\text{O}_2$  electrode during charge. As the Li ion is deintercalated, the Mn XANES spectrum exhibits some changes in the shape of the edge due to changes in the Mn local environment but does not show a shift to higher energy values. The energy position and the shape of these spectra are very similar to those of the  $\text{Li}_{1.2}\text{Cr}_{0.4}\text{Mn}_{0.4}\text{O}_2$  electrode material, in which manganese remains as  $\text{Mn}^{4+}$  throughout charge and discharge.<sup>7,8</sup> This provides clear evidence that most of Mn ions in pristine  $\text{LiNi}_{0.5}\text{Mn}_{0.5}\text{O}_2$  are already in the  $\text{Mn}^{4+}$  oxidation state and are not oxidized as a result of the Li de-intercalation. In contrast, the Ni edge continuously shifts to higher energy values on charging. A comparison of these spectra with that of the  $\text{Ni}^{3+}$  reference material  $\text{LiNiO}_2$  (plotted in Fig. 3b), indicates that the average oxidation state for nickel is below 3+ for the pristine material, gradually increasing to above 3+ at 4.6 V, which was the highest voltage used in this study. Quantitative analysis of the oxidation states of Ni will be published later with data collected at the fully charged state.

The selected normalized Mn and Ni K-edge XANES spectra of  $\text{LiNi}_{0.5}\text{Mn}_{0.5}\text{O}_2$  electrode during discharge are given in Figure 4 (a) and (b) respectively. No significant energy shift can be observed in the Mn XANES spectra up to scan 25, which corresponds to a discharged state slightly above the 1-volt plateau (approx. 1.2 V). The Mn edge started to move to lower energy as the 1-volt plateau was approached (scan 26) and continued to shift as the discharge was continued. This is clearly reflected in the difference between scans 29 and 35. In contrast, the Ni edge shifts gradually to lower energies on discharging at higher voltages, reaching its original position at around scan 27 (1.3 V), where it remains essentially unchanged throughout the 1-volt plateau discharge. This indicates that the  $\text{Ni}^{2+}/\text{Ni}^{4+}$  redox reaction in this system is reversible and that the capacity obtained in the 1-volt plateau is due to the reduction of  $\text{Mn}^{4+}$ , consistent with the report of Johnson et al.<sup>4</sup>

The Mn and Ni K-edge XANES results during first charge and discharge at potentials near 4 V indicate that charge compensation in the cathode material is achieved mainly via the oxidation/reduction of  $\text{Ni}^{2+}$  and  $\text{Ni}^{4+}$  ions, in agreement with earlier predictions<sup>9</sup> and recent 1<sup>st</sup> principles calculations.<sup>10</sup> In contrast, the Mn ions do not appear to actively participate in the charge compensation process, remaining largely unchanged in the  $\text{Mn}^{4+}$  oxidation state. This is consistent with suggestions that the stability of these layered materials, and the suppression of the layered-to-spinel transformation, is at least in part, due to the absence of  $\text{Mn}^{3+}$  ions, during cycling at potentials of approximately 4V.<sup>10</sup>

Figure 5 shows Fourier transform magnitudes of the Mn and Ni K-edge EXAFS spectra during charge. The first coordination shell consists of oxygen, while the peak feature due to the second coordination shell is dominated by the nickel and manganese cations. The most significant change during charge is observed in the first coordination shell around Ni atoms. The dramatic changes of the first coordination peaks during charge indicate that the charge compensation mainly occurs at the Ni sites and results in a significant decrease in the average Ni-O bond length.

**Conclusions:** We have investigated the evolution of the local electronic and atomic structure of the  $\text{LiNi}_{0.5}\text{Mn}_{0.5}\text{O}_2$  electrode using *in situ* Mn and Ni K-edge XAS techniques during the first charge and discharge process. From the Mn and Ni K-edge XANES results, we conclude that the charge compensation, when charging between 2 and 4.6 V, is achieved mainly by the oxidation of  $\text{Ni}^{2+}$  to  $\text{Ni}^{4+}$  ions, while the manganese ions remain mostly unchanged in the  $\text{Mn}^{4+}$  state. The EXAFS results are consistent with these conclusions. When discharging at low voltage plateau (~1 V), however, the charge compensation for the Li-ion electrochemical process is achieved via reduction of  $\text{Mn}^{4+}$ .

**Acknowledgments:** The XAS measurements were carried out at Beam Line X18b at NSLS. The work performed at SUNY Stony Brook was supported by the National Science Foundation (DMR 9901308) and SUNY Stony Brook, via a joint USB/BNL grant. The work carried out at BNL was supported by the Assistant Secretary for Energy Efficiency and Renewable Energy, Office of Transportation Technologies, Electric and Hybrid Propulsion Division, USDOE under Contract Number DE-AC02-98CH10886.

#### References:

1. T. Ohzuku and Y. Makimura, *Chemistry Letters*, 744 (2001).
2. Z. Lu, D. D. MacNeil, and J. R. Dahn, *Electrochem. Solid-State Lett.*, **4**, A191 (2001).
3. J.-S. Kim, C. S. Johnson, and M. M. Thackeray, *Electrochem. Commun.* **4**, 205 (2002).
4. C. S. Johnson, J.-S. Kim, A. J. Kropf, A. Kahaian, J. T. Vaughey, and M. M. Thackeray, *Electrochem. Commun.* **4**, Available online on April 30 (2002).
5. M. Balasubramanian, X. Sun, X. Q. Yang, and J. McBreen, *J. Power Sources*, **92**, 1 (2001).
6. R. J. Gummow, M. M. Thackeray, W. I. F. David, and S. Hull, *Mater. Res. Bull.*, **27**, 327 (1992).
7. M. Balasubramanian, J. McBreen, I. J. Davidson, P. S. Whitfield, and I. Kargina, *J. Electrochem. Soc.*, **149**, A176 (2002).
8. B. Ammundsen, J. Paulsen, I. Davidson, R. S. Liu, C. H. Shen, J. M. Chen, L. Y. Jang, and J. F. Lee, *J. Electrochem. Soc.*, **149**, A431 (2002).
9. B. Ammundsen and J. Paulsen, *Adv. Mater.*, **13**, 943 (2001).
10. Reed and G. Ceder, *Electrochem. Solid-State Lett.*, **5**, A145 (2002).

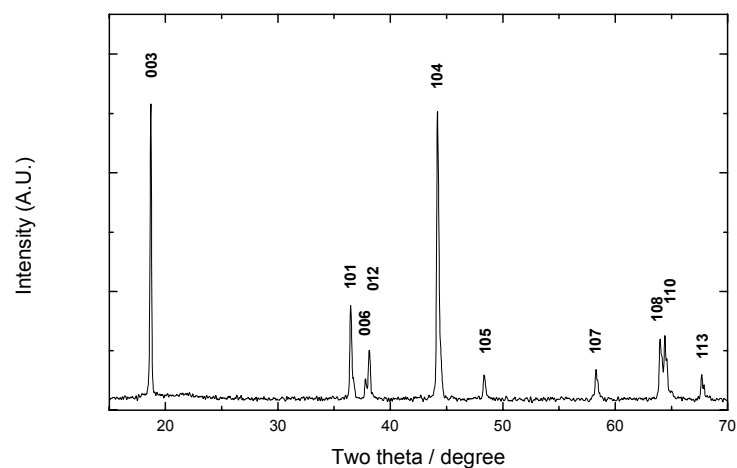


**Figure 1.** XRD pattern of  $\text{LiMn}_{0.5}\text{Ni}_{0.5}\text{O}_2$

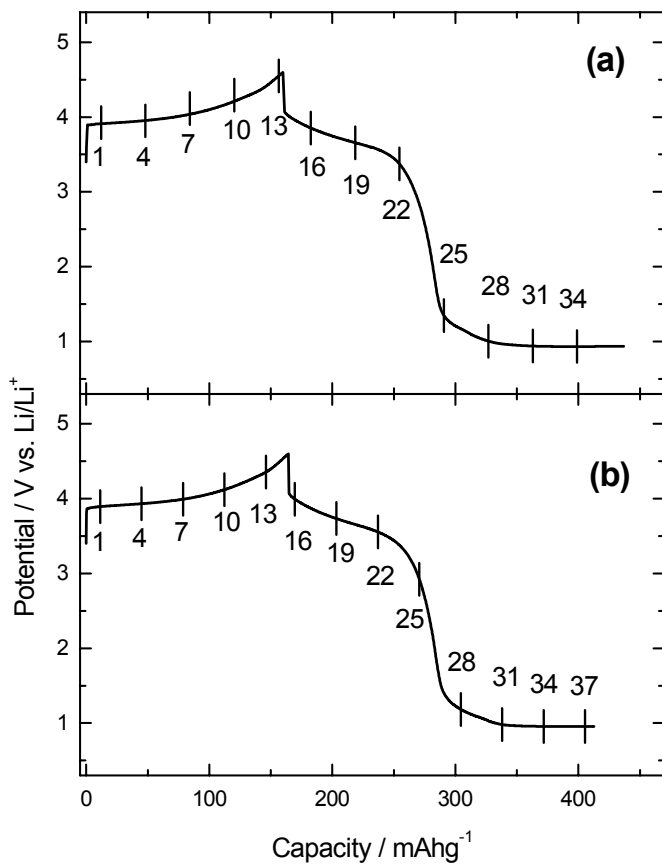


**Figure 2.** Voltage profiles during the first charge and discharge; (a) cell for the Mn XAS, (b) cell for the Ni XAS. Every third XAS scan is marked on the curves.

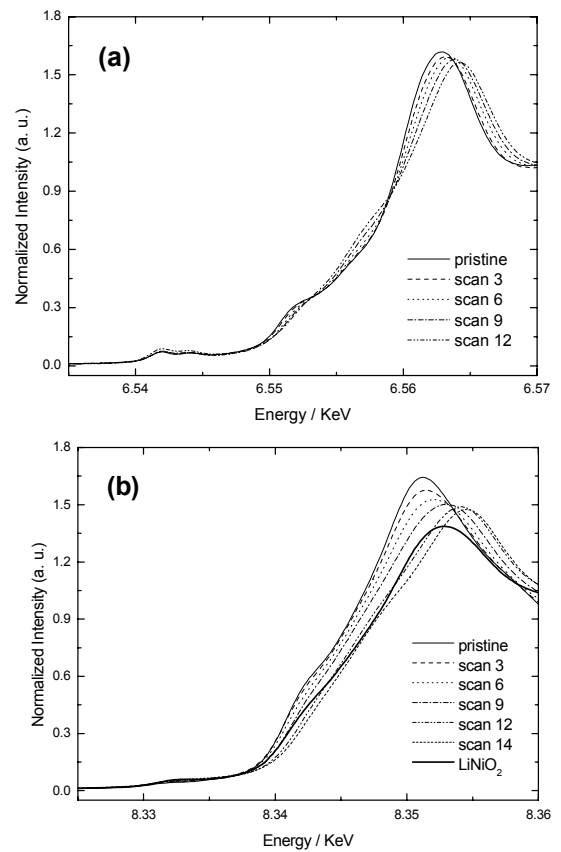


**Figure 3.** Normalized (a) Mn K-edge and (b) Ni K-edge XANES spectra during charge. The spectrum of LiNiO<sub>2</sub> is included as a standard in (b).

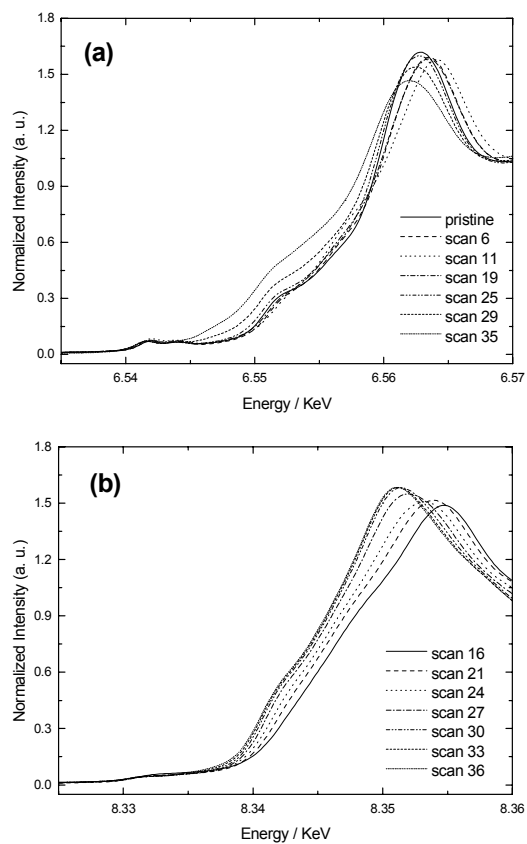


**Figure 4.** Normalized (a) Mn K-edge and (b) Ni K-edge XANES spectra during discharge.

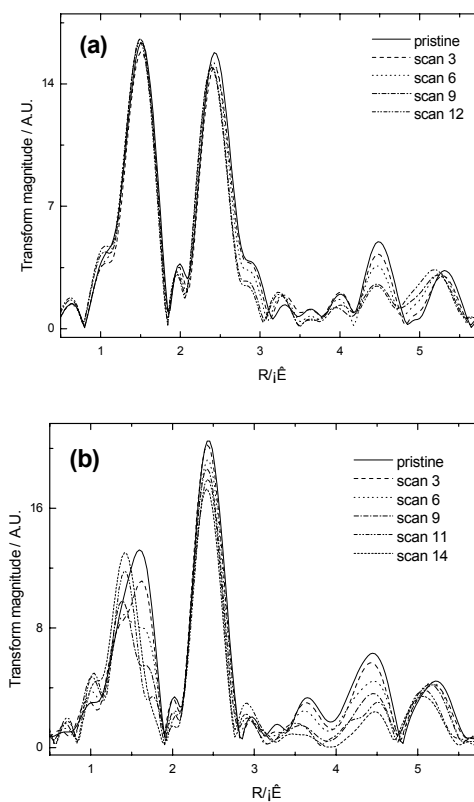


**Figure 5.**  $k^3$ -weighted Fourier transform magnitudes of (a) Mn K-edge and (b) Ni K-edge EXAFS spectra during charge.